WARSAW UNIVERSITY OF TECHNOLOGY Index 351733
FACULTY OF CIVIL ENGINEERING
COMMITTEE FOR CIVIL AND WATER ENGINEERING
POLISH ACADEMY OF SCIENCES ISSN 1230-2945

DOI: 10.24425/ace.2026.157464

ARCHIVES OF CIVIL ENGINEERING

Vol. LXXII ISSUE 1 2026

pp. 121 –133

Research paper

Research on stability analysis and treatment measures of high fill slope

Jianpei Li[1], Dong Yang[2], Yuanyuan Li[3]

Abstract: With the rapid development of China's transportation industry, the treatment of high fill slopes in mountainous regions urgently needs to be addressed. There were many factors that contribute to slope instability, but most slope failures are caused by ineffective treatment of the fill soil, leading to poor internal drainage and the formation of weak soil layers in the slope, which are prone to large deformation and instability. An analysis was conducted on a high fill slope at an airport in Sichuan before and after reinforcement, monitoring the slope's deformation and displacement. Additionally, FLAC3D finite element simulation software was used to perform a simulation analysis under the most unfavorable conditions. By comparing the analysis results with the actual engineering project, it was found that using a comprehensive treatment method to support the high fill slope significantly improves its stability, providing a reference for similar projects in the future.

Keywords: high fill slope, slope instability, monitor, deformation displacement

[1]B.Sc., Henan Quality Institute, Pingdingshan, 467000, China, e-mail: l63523129@126.com, ORCID: 0009-0004-5846-5924
[2]MSc., Henan Quality Institute, Pingdingshan, 467000, China, e-mail: 912897411@qq.com, ORCID: 0009-0000-1240-4852
[3]MSc., Henan Quality Institute, Pingdingshan, 467000, China, e-mail: 735973221@qq.com, ORCID: 0009-0003-2473-9598

1. Introduction

With the development of the economics, there is an increasing amount of infrastructure construction, and some projects are located in complex terrains, especially in mountainous areas where many high fill slopes exist. If these slopes are not properly treated, they can seriously endanger the safety of the projects. There are many methods for dealing with high fill slopes, including soil backfill, installing retaining walls, bolt-shotcrete support, and adjusting the slope ratio.

Analyzed the supporting effect of anchor lattice beams on slopes at different anchoring angles [1], lengths, and spacing through a combination of experimentation and simulation, and obtained the optimal supporting method. Discusses the reconnaissance of the substrate structure in an area threatened by mass movements along a modernized section of a railway line [2]. The results indicate that an integrated approach, combining geophysical imaging and geotechnical reconnaissance, allows for a detailed understanding of the structure and lithology of landslide areas. The study adopted an advanced strength double reduction coefficient method for slope stability analysis [3], which considers the different influence weights of cohesion and internal friction angle, and reduces them with different reduction coefficients to describe the stability of the slope. Semi-analytical solutions are proposed for calculating pore-water pressure distributions and slope stability in an infinite multi-layered slope considering both hydrological and mechanical effects of vegetation, the derived solutions can be used to guide engineering practices of vegetated slope and landfill cover [4].

It is crucial to understand the factors contributing to slope instability. Systematic review examines the factors influencing slope instability [5], the role of climatic conditions, and the impact of agricultural practices in the region. Using the PRISMA framework, 105 studies from 2000 to 2023 were analyzed, identifying key trends and research gaps through bibliometric and thematic analyses. The stability analysis results are presented in dimensionless stability charts [6], the safety measures for slopes are greatly dependent on the Geological Strength Index and the slope geometric 3D effects. A closed-form solution for concave open pit slopes is proposed through regression analysis. Study presents an integrated approach to landslide early warning and vulnerability assessment in the Tijuana Coastal Region by combining geotechnical monitoring, remote sensing [7], and Internet of Things (IoT) technologies. A slope stability analysis method based on the known seepage lines is proposed [8]. the slope stability analysis method based on known seepage lines is applied to a certain tailings dam project. The influence of vegetation root system characteristics [9], on the stability of loess slopes subjected to rainfall infiltration is investigated using a finite element model developed in COMSOL®, which couples seepage and mechanical behavior. Focuses on the engineering background of the Zhongmei Pingshuo Anjialing Open pit Mine and employs a combination of theoretical analysis [10], laboratory experiments, and industrial applications to investigate the overburden movement as a driver of slope instability and sliding, and its control.

With the advancement of big data technology, the application of finite element software in slope engineering has significantly enhanced the convenience of slope monitoring and construction. This paper addresses the solution of slope stability problems in 3D using the finite element method and incremental procedures like the shear strength reduction or limit

load 1 methods [11]. Through deterministic and probabilistic stability analyses of a slope with high FS and stable for many years [12], that the variability inherent to local materials results in low-reliability levels, indicating a higher risk of slope failure, even though the FS obtained in deterministic analyses is high, providing guidelines for future research and engineering practices. Provide a practical and optimal multistage slope design for rock mass excavation [13]. The FLAC3D commercial software was used for numerical simulation, and the multi-verse optimization (MVO) algorithm was applied to design the optimal multistage slope. the resulting design was subsequently implemented in slope engineering. Recorded displacements confirmed that the optimal design is practical and can suitable for engineering applications. This study employs literature review, theoretical analysis, software development [14], and numerical simulation methods to explore the application of BIM models in slope stability analysis. Focuses on a power transmission and transformation project in Huizhou City [15], Guangdong Province. using MIDAS 2019, an unsaturated seepage-mechanics coupling model was established to systematically investigate the influence of slope ratios on slope stability under rainfall conditions and the reinforcement effects of anti-slide piles. Using the Hanshankou tunnel as an engineering case [16], the deformation and force occurring during the entire construction process of the tunnel-slope system were monitored. Based on specific engineering, this paper analyzes the types of deformation and influencing factors of high fill slopes, studies the effect of slope reinforcement, and proposes reinforcement schemes, providing a reference for similar projects in the future.

2. Failure types of high embankment slopes and project overview

2.1. Types of deformation high embankment slopes

The deformation and instability of high embankment slopes can be classified into three types based on the mode of instability: settlement of the fill material, shrinkage of the high embankment slope, and settlement of the foundation. The specific manifestations are shown in Fig. 1.

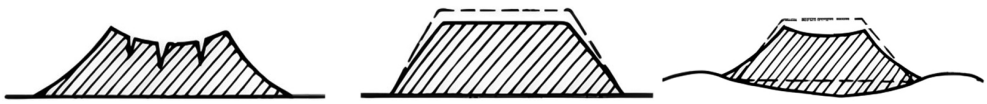

(a) (b) (c)

Fig. 1. Settlement of the fill material: (a) Settlement of the Fill Material; (b) Shrinkage of the Fill Material; (c) Settlement of the Foundation

2.2. Project overview

A certain airport in Sichuan is located on the eastern slope of a basin at an altitude of 3,500 meters. The slope inclines towards the northwest with an angle ranging from 8° to 14°. The terrain forms a large slope of 20° to 60° from west to east. The basin has an open topography and belongs to a Quaternary fault depression basin in terms of geological structure. The western part of the basin is a plateau region with an average altitude of 4,000 to 4,200 meters, while the eastern part is a deeply incised mountainous region with an average altitude of 3,600 to 4,000 meters. To the north, there is a rock peak with an altitude of 5,010 meters, and there are high fill areas present. The airport is located in the alpine monsoon climate zone on the eastern edge of the Tibetan Plateau, where extreme cold weather is frequent, with the lowest temperature dropping to minus 25°C, and the frost period lasting for half a year. The airport is situated on a north-south seismic zone in China, with a historical record of strong seismic activity. The topographic and geomorphic map of the airport is shown in Fig. 2.

Fig. 2. Topography and landform of fill slope

The area has an average elevation ranging from 4,000 to 4,200 m. At its northern end lies Xiaoxitian in the clearance zone, with a summit elevation of 4,033.4 m. The eastern side of the basin features a deeply incised mountainous region, with an average elevation between 3,600 and 4,000 m, characterized by a steep slope gradient varying from 20° to 60° from west to east. The airport is situated at an elevation of 3,447 m, with the overall slope tilting southward at an inclination angle of 8° to 14°. The maximum seismic intensity in the project area is 7 degrees.

3. Slope deformation monitoring

3.1. Monitoring of the original high fill slope

Due to the unique geographical location of the fill slope, cracks were observed on the eastern top of the slope during monitoring. It took a total of 3 days for the cracks to develop from their initial appearance at the rear edge to full connection. The width of the cracks reached

about 5 cm, with a visible depth of over 1 m and a length of 141 m. The area enclosed by the cracks exceeded 3,000 m^2. The development process of the cracks on the fill slope is shown in Fig. 3, the width change curve of the rear edge cracks is shown in Fig. 4.

Fig. 3. Trailing edge crack

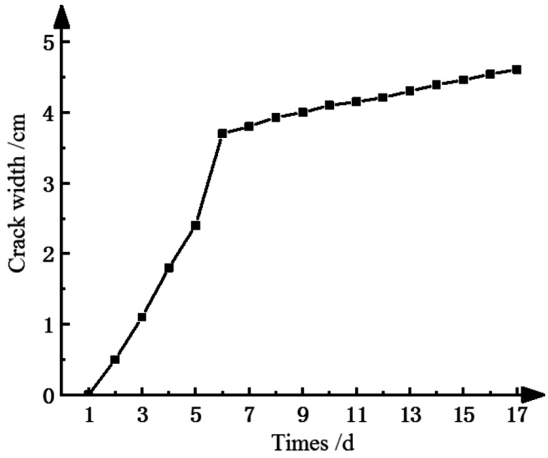

Fig. 4. Trailing edge crack width variation curve

Slope surface displacement monitoring was conducted on the fill slope, with a total of 16 monitoring points arranged in 4 rows. The rows were designated as P1, P2, P3, and P4 from top to bottom. The monitoring frequency was once a week, with a total of 7 monitoring sessions. The horizontal and vertical displacements of each monitoring point are shown in Table 1. The Pythagorean theorem was used to organize the horizontal and vertical displacements, and the average total displacement of each row of the slope was calculated separately. The resulting change chart of the total displacement of the original slope is shown in Fig. 5.

Table 1. Measurement point displacement value

		Horizontal displacement (cm)							Vertical displacement (cm)						
Number of times (m)		1	2	3	4	5	6	7	1	2	3	4	5	6	7
P1	1	0.00	0.29	0.43	0.79	1.06	1.13	1.42	0.00	0.17	0.24	0.40	0.75	0.79	1.11
	2	0.00	0.35	0.56	0.84	1.08	1.24	1.44	0.00	0.13	0.26	0.41	0.68	0.76	0.95
	3	0.00	0.41	0.54	0.79	1.05	1.22	1.52	0.00	0.11	0.24	0.43	0.71	0.79	0.92
	4	0.00	0.36	0.61	0.78	1.08	1.18	1.38	0.00	0.16	0.21	0.38	0.65	0.73	1.01
P2	5	0.00	0.76	1.10	1.37	1.92	2.16	2.31	0.00	0.14	0.46	0.81	1.08	1.24	1.63
	6	0.00	0.78	0.98	1.38	1.88	2.03	2.19	0.00	0.19	0.46	0.83	1.12	1.37	1.56
	7	0.00	0.68	0.99	1.42	1.83	2.06	2.24	0.00	0.18	0.43	0.79	1.17	1.28	1.52
	8	0.00	0.94	1.03	1.34	1.94	2.11	2.26	0.00	0.24	0.51	0.85	1.06	1.34	1.54
P3	9	0.00	1.36	2.42	3.11	3.58	4.09	4.51	0.00	0.36	0.91	1.58	2.38	2.91	3.34
	10	0.00	1.33	2.45	3.15	3.54	4.12	4.52	0.00	0.41	0.88	1.65	2.43	2.89	3.24
	11	0.00	1.42	2.68	3.21	3.61	4.06	4.47	0.00	0.38	0.95	1.84	2.38	2.76	3.38
	12	0.00	1.38	2.64	3.28	3.58	3.94	4.44	0.00	0.44	1.12	1.78	2.46	2.76	3.35
P4	13	0.00	1.99	3.88	4.33	5.14	5.96	6.32	0.00	0.91	1.42	2.45	3.02	3.64	4.25
	14	0.00	1.97	3.75	4.29	5.18	5.84	6.48	0.00	0.86	1.46	2.46	2.96	3.53	4.13
	15	0.00	2.05	3.72	4.51	5.29	5.92	6.31	0.00	0.96	1.58	2.78	3.42	3.85	4.26
	16	0.00	2.01	3.68	4.33	5.16	5.81	6.36	0.00	1.04	1.52	2.69	3.67	4.04	4.68

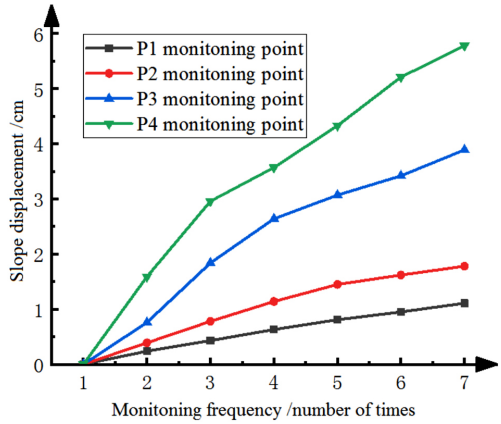

Fig. 5. Diagram of total displacement variation of the original slope

Based on Fig. 5, it can be seen from the sixth monitoring result that the total displacement of P4 has exceeded 5 cm, indicating significant deformation of the slope. This is a noticeable increase in displacement, suggesting that the slope has undergone considerable deformation. The stability of the slope is decreasing, posing potential safety risks, and support measures need to be taken. One measure is to add anchor rods or cables. By installing anchor rods or cables inside the slope, additional tensile strength can be provided to enhance the stability of the slope. Another option is to construct retaining walls or anti-slide piles. Retaining walls or anti-slide piles can be built at the bottom or sides of the slope to resist the sliding force. Additionally, increasing drainage facilities is crucial. Ensuring good drainage of the slope can reduce soil softening and deformation caused by water accumulation. Slope reinforcement is another approach. The slope soil can be reinforced through grouting, reinforcement, and other methods to improve its overall strength. Lastly, a monitoring and early warning system should be established. More monitoring points for displacement, stress, strain, etc., should be set up on the slope to monitor the deformation in real-time, and an early warning system should be established to detect and respond to issues promptly. For slope stability analysis, other factors such as geological conditions, rainfall, groundwater level, etc., also need to be considered. Therefore, in practical engineering, it is recommended to conduct a comprehensive analysis combining multiple monitoring data and geological information to develop an effective slope management plan.

3.2. Monitoring of reinforced high fill slope

Based on the characteristics of the high slope near the airport, three treatment plans are proposed.

Plan 1: Completely remove the deformed soil and then perform backfill treatment;

Plan 2: Install anti-slide supports on the sliding slope and then fill the soil;

Plan 3: Implement comprehensive treatment for the unstable slope, partially remove the original slope soil, install a reinforced earth retaining wall and reinforce the foundation, backfill soil behind the wall, and lay steel wire mesh on the top.

It demonstrates structural stability, as the reinforced earth retaining wall combined with foundation reinforcement can effectively resist the sliding thrust of the slope. Compared to Plan 1, which involves complete removal and back filling (requiring substantial earthwork), and Plan 2, which relies on anti-slide supports (necessitating high-strength materials), Plan 3 reduces material costs through partial removal of the original slope soil and optimized back filling. Additionally, it offers construction feasibility by allowing phased implementation, thereby avoiding the risk of secondary slope failure caused by large-scale excavation. After comparing the plans, the comprehensive treatment shows significant advantages in terms of construction duration and cost, and it is also convenient for controlling the deformation of the high fill slope. Therefore, Plan 3 is ultimately selected. Based on the different types of slip zones observed on site, the mechanical properties of the soil in both natural and saturated states are determined, as shown in Table 2.

The slide mass is predominantly composed of plain fill, with silt only exposed in localized sections. Therefore, the natural and saturated unit weights of the slide mass are determined based on the primary stratum of plain fill, with values taken from the results of previous

investigations. Indoor tests indicate that the natural unit weight of the plain fill within the slide mass is 21.62 kN/m^3, while the saturated unit weight is 23.13 kN/m^3. Thus, the adopted values for the slide mass soil are: natural unit weight of 21.64 kN/m^3 and saturated unit weight of 23.15 kN/m^3.

Table 2. Mechanical parameters of soil layers under different sliding zone conditions

Different slip zone conditions	**Native state**		**Saturation condition**	
	***C* (kPa)**	**φ (°)**	***C* (kPa)**	**φ (°)**
Fill soil + vegetative layer	9.1	9.6	8.2	8.6
fill + pebble	5.6	18.2	4.9	16.8
fill + silt	12.1	12.8	11.8	11.2
fill + silty clay	12.9	11.9	12.1	11.3

Based on the on-site soil conditions, the comprehensive treatment plan is specifically divided into the following three steps. (1) Perform slope cutting on the unstable and deformed parts of the original slope to reduce the accumulated load on the upper part of the slope. Drainage holes are set at the toe of the slope to drain the pore water inside the soil; (2) Use reinforced retaining walls to support the upper stable soil. The safe and stable areas can be directly subjected to slope cutting, while other areas are reinforced by laying steel wire mesh. The fill soil should not be located in the cracks of the deformed soil, and reinforced retaining walls are used for supporting and protection at the toe of the fill slope; (3) Partially replace the foundation soil of the retaining wall with pebble material, and use high-pressure jet grouting piles to support the foundation base of the retaining wall and the backfill soil in front of the wall. The comprehensive treatment plan employs a combination of measures, including slope cutting for the deformed mass, reinforced soil retaining wall construction, grouting treatment, and the establishment of a reflective net protection zone, as illustrated in Fig. 6.

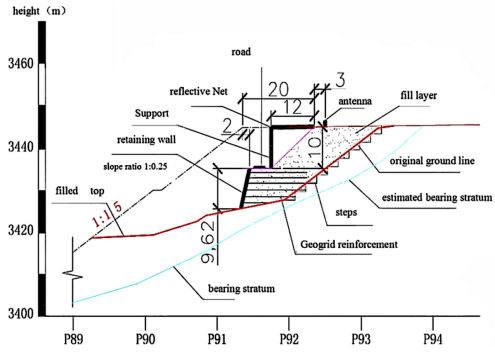

Fig. 6. Slope support design scheme

Displacement monitoring was conducted on the high fill slope after the comprehensive treatment. The vertical positions of the monitoring points were the same as those of the original slope monitoring points, and the monitoring frequency was also kept consistent. The rows were designated as P'1, P'2, P'3, and P'4 from top to bottom. The total displacement of the slope monitoring was calculated, and the average total displacement of each row was taken as the slope surface displacement. the monitoring displacement graph is shown in Fig. 7.

Comparing the total displacement changes before and after slope reinforcement shown in Fig. 7. The calculations before and after slope cutting are presented in Table 3 and Table 4, respectively. the comprehensive treatment plan has achieved good results in addressing the unstable slope. The maximum displacement change is nearly one-third of that of the original slope. Based on the analysis results of the displacement monitoring images, the effectiveness of the treatment measures can be further assessed, and decisions can be made on whether further measures are needed to ensure the long-term stability of the slope. In addition, regular displacement monitoring should continue to be conducted to monitor the stability of the slope and take appropriate maintenance or repair measures when necessary. Displacement monitoring of the high fill slope after comprehensive treatment was very important, as it helps to evaluate the effectiveness of the treatment measures and the long-term stability of the slope.

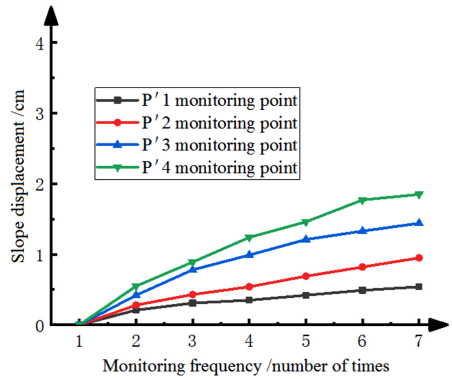

Fig. 7. Diagram of total displacement variation of reinforced slope

Table 3. Calculation table of slope stability and residual sliding force of profile – before slope cutting treatment

Slippery surface number	Computational item	Working condition of calculation		
		I	II	III
H-1	stability coefficient /K	1.34	1.16	1.11
	surplus sliding force (kN/m)	0	0	0
H-2	stability coefficient /K	1.31	1.12	1.07
	surplus sliding force (N/m)	0	0	0

Note: For the H-1 slip surface, it is considered that shearing occurs through the middle of the jet grouting piles; for the H-2 slip surface, it is considered that shearing occurs at the bottom of the jet grouting piles. The above calculations do not account for the enhancement effect of the jet grouting piles on the soil's shear strength.

Table 4. Calculation table of slope stability and residual sliding force of profile – after slope cutting treatment

Slippery surface number	Computational item	Working condition of calculation		
		I	II	III
H-1	stability coefficient /K	1.42	1.19	1.06
	surplus sliding force (KN/m)	100.15	524.92	0
H-2	stability coefficient /K	1.34	1.16	1.16
	surplus sliding force (KN/m)	80.64	571.55	0

Note: For the H-1 slip surface, it is considered that shearing occurs through the middle of the jet grouting piles; for the H-2 slip surface, it is considered that shearing occurs at the bottom of the jet grouting piles. The above calculations do not account for the enhancement effect of the jet grouting piles on the soil's shear strength.

4. Numerical simulation analysis

To verify the feasibility of the above support method. FLAC3D finite element software was used for the simulation, and a comparative analysis was performed with the specific engineering project. Given the complexity of the slope, an idealized model of the slope was simulated and analyzed, with the model diagram shown in Fig. 8. To better assess the supporting effect of the fill slope, the simulation parameters were adjusted according to the project, and the least favorable mechanical parameters were used for the simulation based on the on-site investigation data, with the parameters listed in Table 5.

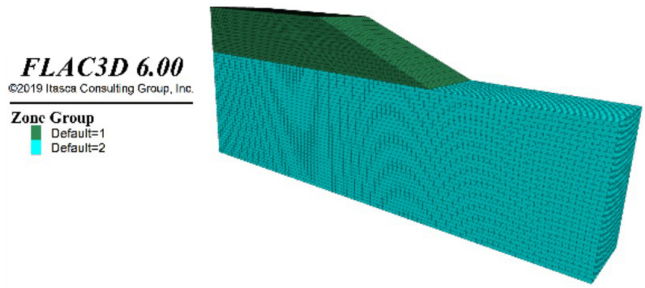

Fig. 8. Model grid division

Table 5. Soil parameter indicators

Serious (kN·m^{-3})	C (kPa)	φ(°)	Bulk modulus (MPa)	Shear modulus (MPa)
21	8	8.5	15	6

Based on the above parameters, a simulation of the slope was conducted, with the results shown in Fig. 9. The slope exhibits a clear landslide zone, and at a calculation ratio of 1e-5, the maximum displacement of the slope was close to 1.3 m, indicating significant instability. However, the simulation and analysis of slope stability are complex processes

that require consideration of various factors and parameters. Therefore, before formulating specific treatment measures, it was recommended to conduct detailed geological surveys, slope stability analyses, and simulations to ensure that the measures taken are effective and safe. Additionally, the treatment and maintenance of slopes were long-term processes that require regular monitoring and evaluation of slope stability, as well as taking necessary measures to maintain their long-term stability.

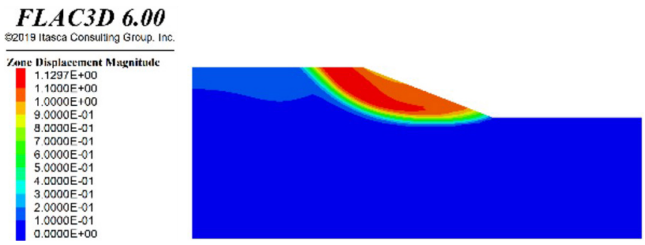

Fig. 9. Original slope displacement cloud map

The original slope was reinforced using Scheme 3 from actual engineering practices. The simulated conditions were consistent with those of the original slope. The displacement contour map of the reinforced slope was shown in Fig. 10. The slope displacement has significantly decreased, with a maximum displacement of 2 cm, and there are no landslide zones, indicating that the slope was in a stable state. By comparing the displacement contour maps before and after reinforcement, it can be seen that the slope stability has significantly improved and the slope displacement has significantly reduced after adopting the comprehensive treatment method for reinforcement, with no appearance of landslide zones.

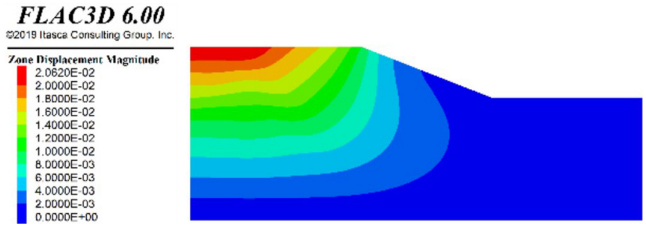

Fig. 10. Reinforcement slope displacement cloud map

Based on the above analysis, the reinforced slope was in a stable state, with significantly reduced displacement and no appearance of landslide zones, indicating that the reinforcement measures were effective and the slope stability has been improved. However, it should be noted that the displacement contour map can only provide displacement information at a specific moment. To comprehensively assess the long-term stability of the slope, long-term displacement monitoring and regular safety evaluations are necessary. In future monitoring and evaluations, it was recommended to continue regular displacement monitoring of the reinforced slope, as well as other relevant safety monitoring, such as stress, strain, and groundwater level. This will help to promptly identify any potential instability factors and take necessary measures for maintenance or repair, ensuring the long-term safety and stability of the slope.

5. Conclusions

The stability of high-fill slopes was crucial for engineering safety. Slope stability was influenced by various factors, including geological conditions, climatic conditions, construction methods, etc. Therefore, detailed stability analysis must be conducted before the design and construction of high-fill slopes to assess their performance under various conditions.

1. Through comprehensive analysis of engineering examples and numerical simulations, it was evident that the effect of using comprehensive treatment methods for supporting high-fill slopes was significant. Under the influence of the same factors, the total displacement of the reinforced slope was significantly less than that of the original slope, greatly enhancing slope stability.
2. By analyzing actual engineering projects with numerical simulation software, the construction simulation results can be intuitively visualized, allowing for advance preparations before construction. This not only expedites the construction schedule but also saves costs while ensuring quality.
3. The stability of high-fill slopes was a long-term process. Even with effective treatment measures in place, long-term monitoring and maintenance of the slopes were necessary. Through long-term monitoring, signs of slope instability can be promptly identified, and necessary measures can be taken for maintenance or repair.
4. When conducting stability analysis and researching treatment measures for high-fill slopes, decisions must be based on scientific data and analysis. This includes using reliable software for simulation analysis, collecting accurate geological and meteorological data, and conducting detailed construction monitoring. Only through science-based decision-making can the safety and stability of slopes be ensured.

References

[1] M.L. Wu, "Research on grouting improvement and anchor rod lattice beam support of mixed fill slopes", M.A. thesis, Hunan University of Technology, Zhuzhou, 2021.

[2] M. Superczyńska, M. Maślakowski, and R. Mieszkowski, "Three-dimensional interpretation of geophysical and geotechnical investigation of landslides", *Archives of Civil Engineering*, vol. 70, no. 4, pp. 99–111, 2024, doi: 10.24425/ace.2024.151882.

[3] Y.C. Gao, Y. Zhao, T.Y. Xu, and J.L. Xu, "Stability analysis of ultra-high and steep reinforced soil fills slopes based on strength reduction", *Archives of Civil Engineering*, vol. 70, no. 2, pp. 417–430, 2024, doi:10.24425/ace.2024.149872.

[4] S. Feng, et al., "Semi-analytical solutions for pore-water pressure distributions and slope stability in an infinite multi-layered vegetated slope considering highly-nonlinear hydraulic properties of soil", *Computers and Geotechnics*, vol. 186, art. no. 107445, 2025, doi: 10.1016/J.COMPGEO.2025.107445.

[5] V.J. Gabriel, R.H. Wang, D. Mahato, and C. Wei, "Slope stability and disaster mechanisms in the Honghe Hani Terraces: a systematic review", *The Egyptian Journal of Remote Sensing and Space Sciences*, vol. 28, no. 3, pp. 411–425, 2025, doi: 10.1016/J.EJRS.2025.06.003.

[6] S.L. Jia, F. Zhang, J. Ji, Z.M. Zhang, and J. Xu, "3D stability and reliability of concave open pit slope in rock with Hoek-Brown strength criterion", *International Journal of Rock Mechanics and Mining Sciences*, vol. 194, art. no. 106190, 2025, doi: 10.1016/j.ijrmms.2025.106190.

[7] K. Ambika, N. Alzaben, A.G. Alghamdi, and S. Venkatraman, "Integrated geotechnical and remote sensing-based monitoring of unstable slopes for landslide early warning using IoT and sensor networks", *Journal of South American Earth Sciences*, vol. 164, art. no. 105666, 2025, doi: 10.1016/J.JSAMES.2025.105666.

[8] M. Weiliang and S. Longtan, "Slope Stability Analysis Method Based on Known Seepage Lines", *International Journal of Geomechanics*, vol. 25, no. 9, art. no. 04025176, 2025, doi: 10.1061/IJGNAI.GMENG-11618.

[9] K.F. Kong, Z.X. Deng, F. Chen, Z. Wang, and Y.L. Chen, "Numerical analysis of the effect of vegetation root reinforcement on the rainfall-induced instability of loess slopes", *Scientific Reports*, vol. 15, no. 1, art. no. 23233, 2025, doi: 10.1038/S41598-025-06400-3.

[10] J.P. Li, W.C. Wang, H.B. Yao, J.J. Yan, and Z.Y. Pei, "Study on the Law and Control Mechanism of Slope Sliding Instability Under Hanging Wall Coal Mining", *Advances in Civil Engineering*, vol. 2025, no. 1, art. no. 7884079, 2025, doi: 10.1155/ADCE/7884079.

[11] S. Sysala, M. Béreš, S. Bérešová, T. Luber, and Z. Michalec, "Advanced continuation and iterative methods for slope stability analysis in 3D", *Computers and Structures*, vol. 315, art. no. 107842, 2025, doi: 10.1016/J.COMPSTRUC.2025.107842.

[12] M. Heidemann, J.V.E. Maximiliano, and L.A. Bressani, "Shear Strength Variability and Slope Stability Risk in Gneissic Residual Soils of Serra do Mar", *Geotechnical and Geological Engineering*, vol. 43, no. 6, art. no. 242, 2025, doi: 10.1007/S10706-025-03202-2.

[13] P.Y. Fan, J.H. Chen, J.W. Chen, X.H. Shen, and M. Wang, "Optimal design of a multistage slope using the multi-verse optimization algorithm", *Scientific Reports*, vol. 15, no. 1, art. no. 6376, 2025, doi: 10.1038/S41598-025-87155-9.

[14] L.Z. Yuan, S.Y. Liu, and L.H. Meng, "Numerical simulation analysis of slope stability from rainwater utilizing the Civil3D+Flac3D coupling", *Desalination and Water Treatment*, vol. 319, art. no. 100517, 2024, doi: 10.1016/J.DWT.2024.100517.

[15] G.L. Huang, et al., "Research on Stability of Transmission Tower Slopes with Different Slope Ratios Under Rainfall Conditions and Reinforcement Effects of Anti-Slide Piles", *Buildings*, vol. 15, no. 12, art. no. 2066, 2025, doi: 10.3390/BUILDINGS15122066.

[16] X.X. Tian, Z.P. Song, Y. Cheng, and J.B. Wang, "Deformation distribution characteristics of a tunnel–slope system and its reinforcement measures", *Bulletin of Engineering Geology and the Environment*, vol. 84, no. 6, art. no. 271, 2025, doi: 10.1007/S10064-025-04297-W.

Received: 2025-04-17, Revised: 2025-08-07